Fig. 1 Hashimoto, *et al.*

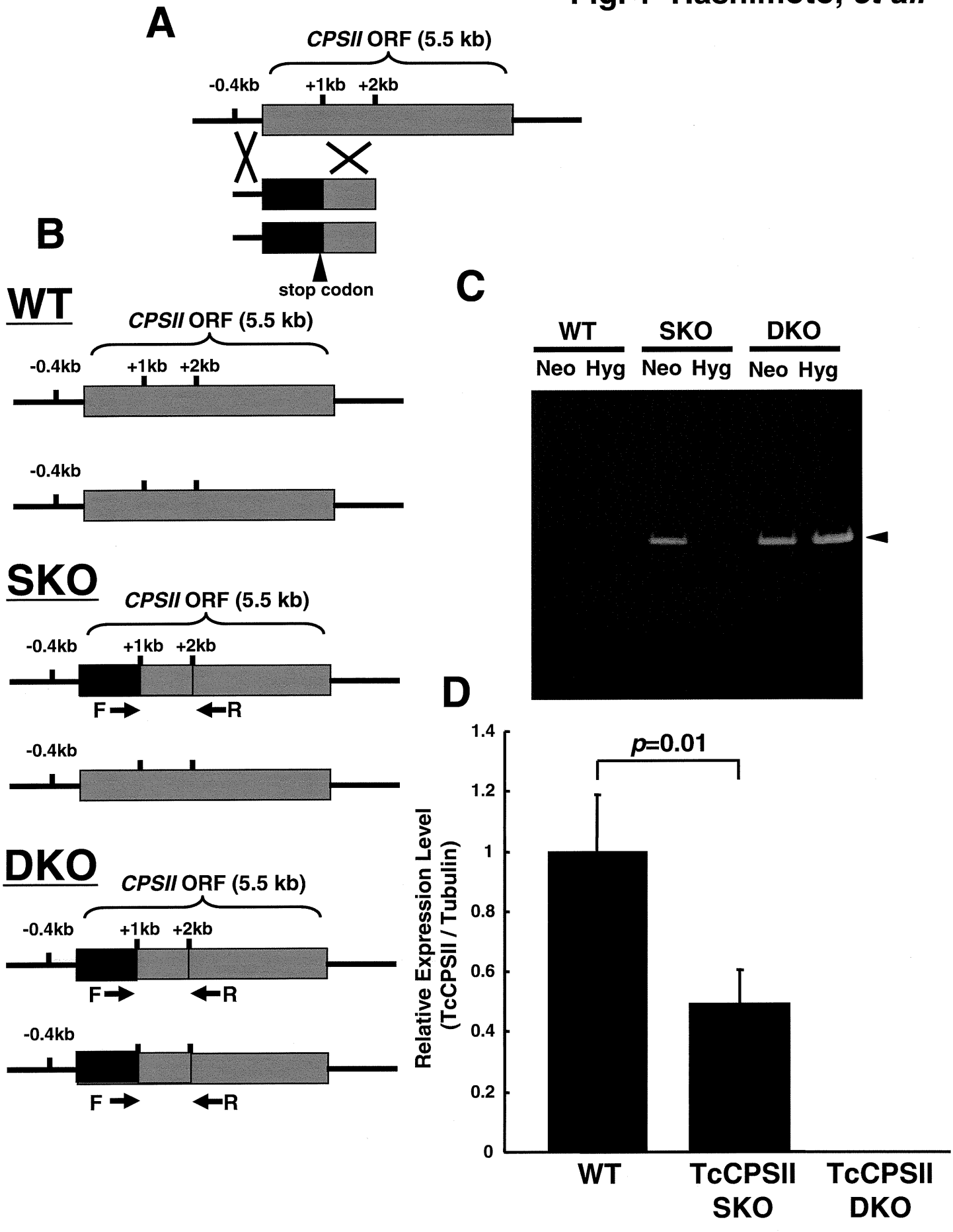

Fig. 2 Hashimoto *et al*

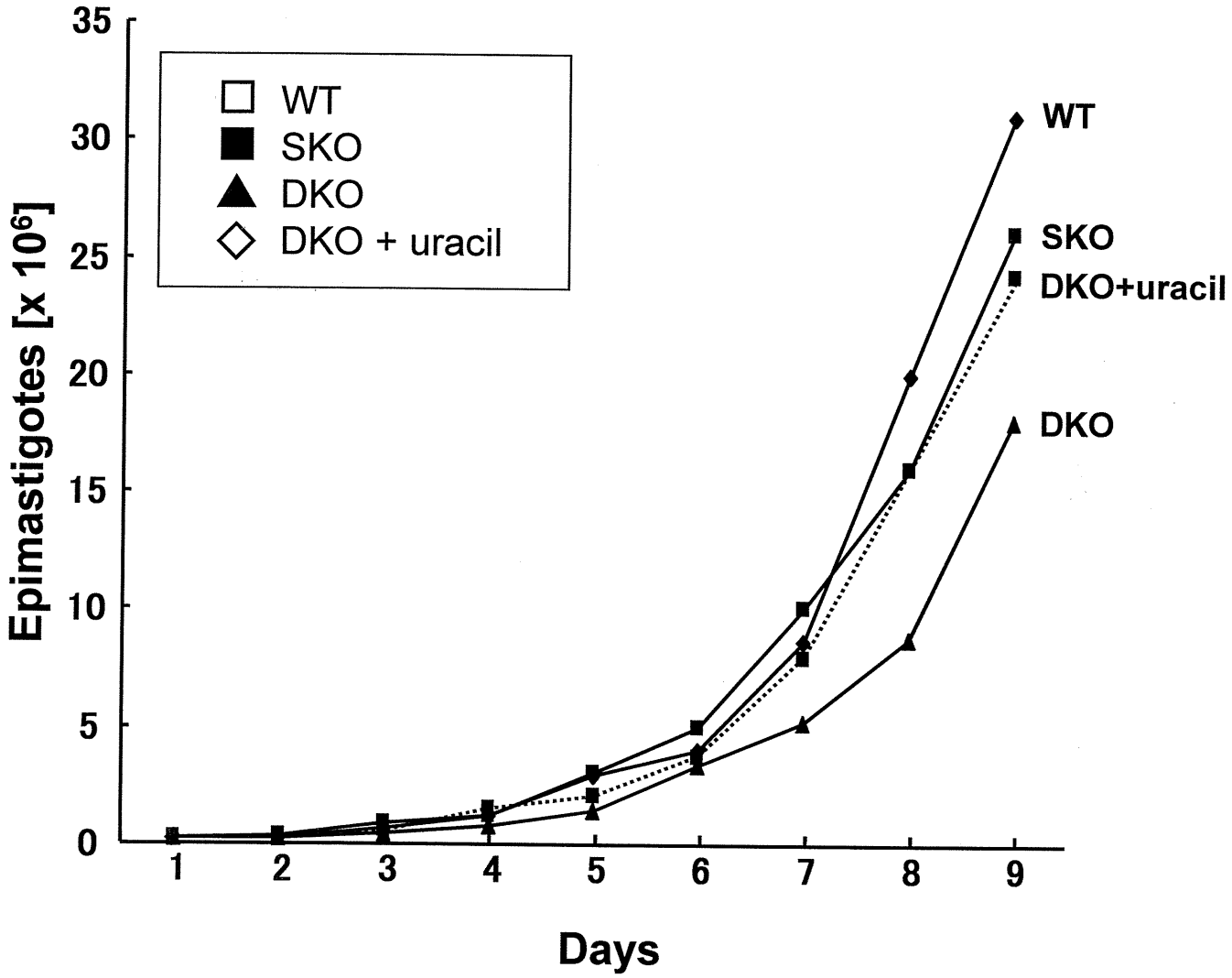

Fig. 3 Hashimoto *et al*

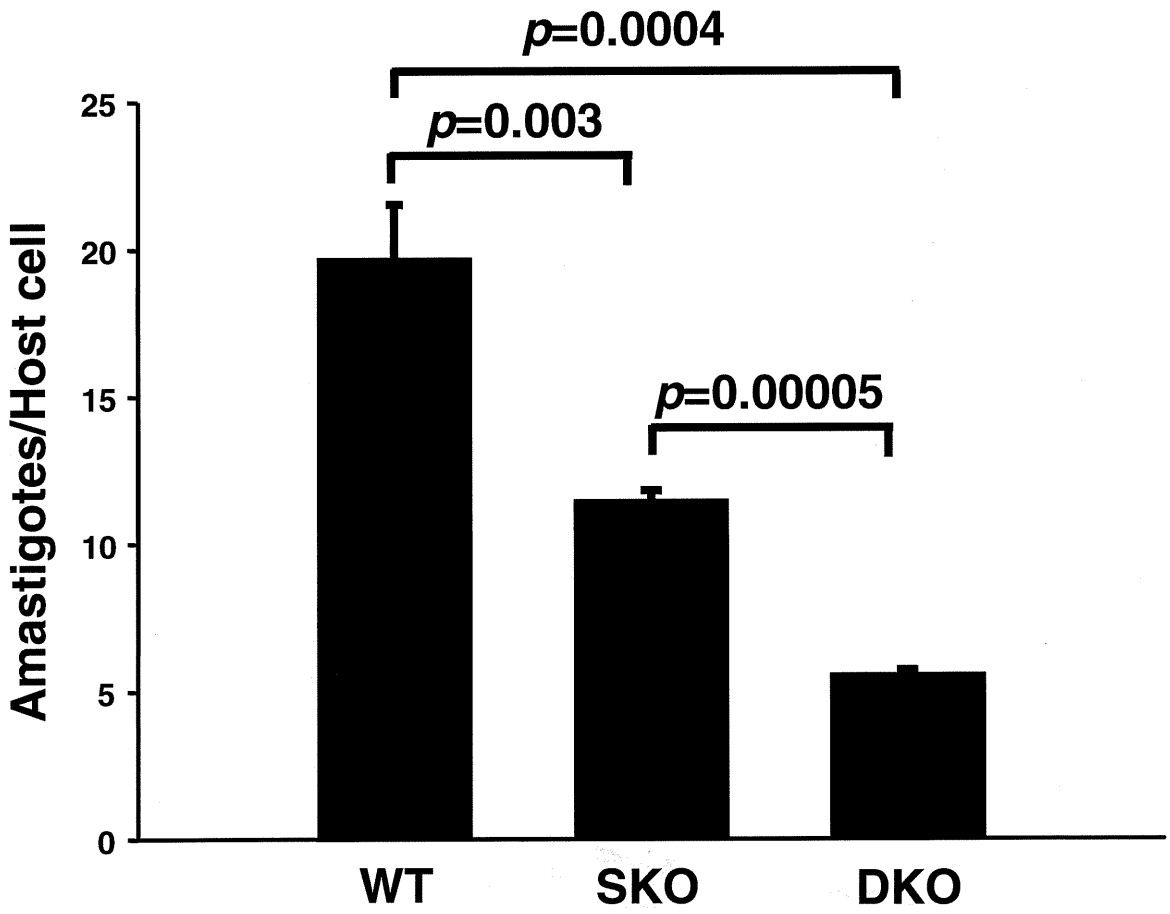

ARTICLE IN PRESS
BBAGEN-27149; No. of pages: 9; 4C: 2, 3, 4, 5, 6, 7
Biochimica et Biophysica Acta xxx (2012) xxx–xxx
Contents lists available at SciVerse ScienceDirect
Biochimica et Biophysica Acta
journal homepage: www.elsevier.com/locate/bbagen

Review

Mitochondrial fumarate reductase as a target of chemotherapy: From parasites to cancer cells☆

Chika Sakai [a], Eriko Tomitsuka [a,b], Hiroyasu Esumi [b], Shigeharu Harada [c], Kiyoshi Kita [a,*]

[a] Department of Biomedical Chemistry, Graduate School of Medicine, The University of Tokyo, Tokyo 113-0033, Japan
[b] Cancer Physiology Project, Investigative Treatment Division, National Cancer Center Research Institute East, 6-5-1 Kashiwanoha, Kasiwa, Chiba 277-8577, Japan
[c] Department of Applied Biology, Graduate School of Science and Technology, Kyoto Institute of Technology, Kyoto 606-8585, Japan

ARTICLE INFO

Article history:
Received 27 July 2011
Received in revised form 28 November 2011
Accepted 17 December 2011
Available online xxxx

Keywords:
Mitochondrial fumarate respiration
Complex II
Hypoxia
Drug target
Ascaris suum
Type II flavoprotein subunit

ABSTRACT

Recent research on respiratory chain of the parasitic helminth, *Ascaris suum* has shown that the mitochondrial NADH-fumarate reductase system (fumarate respiration), which is composed of complex I (NADH–rhodoquinone reductase), rhodoquinone and complex II (rhodoquinol–fumarate reductase) plays an important role in the anaerobic energy metabolism of adult parasites inhabiting hosts. The enzymes in these parasite-specific pathways are potential target for chemotherapy. We isolated a novel compound, nafuredin, from *Aspergillus niger*, which inhibits NADH-fumarate reductase in helminth mitochondria at nM order. It competes for the quinone-binding site in complex I and shows high selective toxicity to the helminth enzyme. Moreover, nafuredin exerts anthelmintic activity against *Haemonchus contortus* in *in vivo* trials with sheep indicating that mitochondrial complex I is a promising target for chemotherapy. In addition to complex I, complex II is a good target because its catalytic direction is reverse of succinate–ubiquionone reductase in the host complex II. Furthermore, we found atpenin and flutolanil strongly and specifically inhibit mitochondrial complex II.
Interestingly, fumarate respiration was found not only in the parasites but also in some types of human cancer cells. Analysis of the mitochondria from the cancer cells identified an anthelminthic as a specific inhibitor of the fumarate respiration. Role of isoforms of human complex II in the hypoxic condition of cancer cells and fetal tissues is a challenge. This article is part of a Special Issue entitled Biochemistry of Mitochondria, Life and Intervention 2010.

1. Introduction

In the general understanding of bioenergetics of higher eukaryotes, oxygen is a most important terminal electron acceptor of mitochondrial respiratory chain (Fig. 1). The major function of the aerobic respiratory chain is the electrogenic translocation of protons out of the mitochondrial or bacterial membrane to generate the proton motive force that drives ATP synthesis by F_oF_1-ATPase. This mechanism of oxidative phosphorylation is conserved basically from aerobic bacteria to human mitochondria. However, recent study on the respiratory chain of the lower eukaryotes which reside micro-aerophilic environment has shown that the mitochondrial NADH-fumarate reductase system (fumarate respiration) plays an important role in the anaerobic energy metabolism [1]. This system is composed of complex I (NADH-quinone reductase), low potential quinone species and complex II (quinol–fumarate reductase: QFR).

Fumarate respiration is well known electron transport chain in the anaerobic bacteria [2]. Reducing equivalent of NADH is transferred to low potential quinone such as naphthoquione by complex I and finally is oxidized by fumarate by the fumarate reductase activity of complex II which is a reverse reaction of succinate–ubiquinone reductase (SQR) activity of complex II. By using this respiratory chain, bacteria are able to synthesize ATP even in the absence of oxygen. Recently our study of parasitic nematode, *Ascaris suum*, showed fumarate respiration also plays an important role in the anaerobic energy metabolism of adult worms, which reside in the host small intestine where oxygen tension is low [1]. Although fumarate reductase activities of bacterial and mitochondrial complex IIs are the same reaction, evolutional positions of each enzyme are quite different. All four subunits of complex II in adult *A. suum* are more closely related to the bacterial and mitochondrial SQR than to bacterial QFR [3–5].

Abbreviations: FRD, fumarate reductase; L3, 3rd stage larvae; LL3, lung stage L3; MK, menaquinone; SDH, succinate dehydrogenase; SQR, succinate–ubiquinone reductase; TCA cycle, tricarboxylic acid cycle; QFR, quinol–fumarate reductase; RQ, rhodoquinone.

☆ This article is part of a Special Issue entitled Biochemistry of Mitochondria, Life and Intervention 2010.

* Corresponding author at: Department of Biomedical Chemistry, Graduate School of Medicine, The University of Tokyo, Hongo, Bunkyo-ku, Tokyo 113-0033, Japan. Tel.: +81 3 5841 3526; fax: +81 3 5841 3444.
E-mail address: kitak@m.u-tokyo.ac.jp (K. Kita).

0304-4165/$ – see front matter © 2011 Elsevier B.V. All rights reserved.
doi:10.1016/j.bbagen.2011.12.013

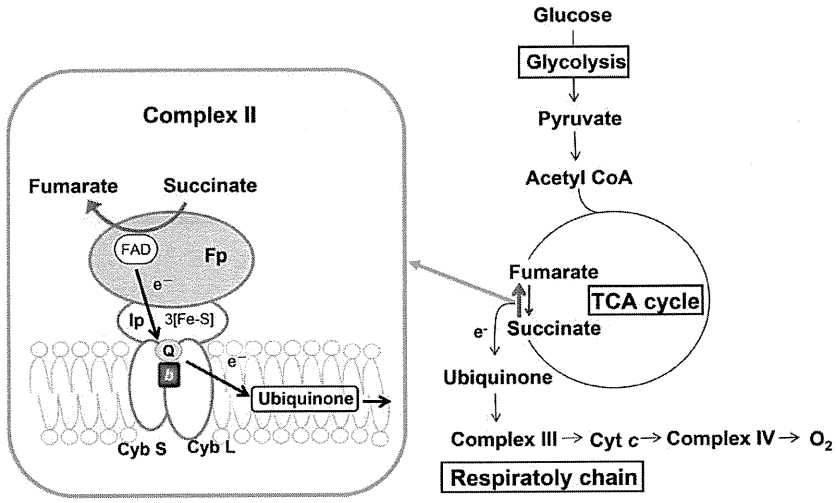

Fig. 1. Complex II is the member of TCA cycle and respiratory chain.Complex II catalyzes the oxidation of succinate to fumarate in the TCA cycle and transports the electron generated by this oxidation to ubiquinone in the respiratory chain. Generally, complex II consists of four subunits. Flavoprotein (Fp) subunit contains a flavin adenine dinucleotide prosthetic group and iron–sulfur protein (Ip) subunit contains three iron–sulfur clusters. There are two hydrophobic cytochrome*b* (Cyb L, Cyb S) subunits. The succinate binding site is located in Fp subunit, while the quinone binding site is formed by three subunits, Ip, Cyb L and CybS. Complex II also catalyzes the reduction of fumarate, a reverse-reaction of succinate dehydrogenase, in the respiratory chain of mitochondria from anaerobic animals, such as *Ascaris suum*, as well as anaerobic bacteria.

Thus, mitochondrial QFR is a new enzyme evolved by "reverse evolution" of SQR rather than direct evolution from bacterial QFR [6].

Recently our study has revealed that fumarate respiration functions in some human cancer cells and supports a survival of cancer cells in low nutrition and low oxygen conditions [7,8]. Furthermore, we found complex II with high QFR activity produces reactive oxygen species (ROS) [9]. ROS has been reported to contribute to proliferation and metastasis of cancer cells via the stabilization of hypoxia-inducible factor-1 (HIF-1) [10]. In addition, succinate produced by fumarate respiration also stabilize HIF-1 by the product inhibition of HIF prolyl hydroxylase, which catalyzes the oxygen-dependent hydroxylation of the conserved proline residues in HIF-1 α [11]. Thus, the relationship between accumulation of succinate resulted from functional defect of human complex II by the mutation of the subunits and carcinogenesis has recently become a focus of research [8].

As fumarate respiration is essential for the growth and survival of the parasites and some cancer cells, it should be a promising target of chemotherapy for both parasitic diseases and cancer. In this review, we focus on recent advances in the study of parasite and human mitochondrial fumarate respiration and complex II which is an important component of the system [8].

2. Fumarate respiration of parasite mitochondria

2.1. Life cycle of A. suum and changes in respiratory chain

A. suum is the most widely known parasite, and has been studied as a representative of human and livestock parasites [12–14]. Because of its large size, *A. suum* is ideal for the study including biochemical analysis. Adult *A. suum* resides in the small intestine of mammals, and the female produces between 200,000 and 400,000 fertilized eggs per day (Fig. 2). Eggs are excreted with feces and become mature eggs containing infectious 3rd stage larvae (L3) in about 2–3 weeks at normal temperature. The eggs reach the small intestine and hatch, when orally ingested by a host. A hatched larva invades the intestinal wall, and migrates to the liver, lung, trachea, and pharyngeal region, and finally returns to the intestine via the esophagus and stomach, and becomes an adult worm. In humans, the larvae of *A. suum* migrate to several organs including liver and lung and cause a wide variety of nonspecific symptoms such as general malaise, cough, liver dysfunction, hypereosinophilia with hepatomegaly and/or pneumonia. The oxygen concentration of the small intestine (~5%) is approximately 25% of that outside the body, and provides an environment of low oxygen tension in which the energy metabolism of the adult differs considerably from that of the larvae and the host (Fig. 3). The phosphoenolpyruvate carboxykinase (PEPCK)–succinate pathway, an anaerobic glycolytic pathway, operates in the adult worm, producing ATP under such a hypoxic conditions. This system is used by many other parasites such as *Echinococcus multilocularis* [15], and has also been observed in the adductor muscle of oysters and other bivalves that require energy conversion under anaerobic conditions. It is therefore considered to be a very common pathway for energy metabolism in adaptation to hypoxic environment [16,17].

The first half of the PEPCK–succinate pathway is the same glycolytic pathway found in mammals, in which phosphoenolpyruvate (PEP) is produced. In contrast to aerobic metabolism in mammals involving the conversion of PEP to pyruvate by pyruvate kinase, the *A. suum* adult fixes CO_2 with PEPCK to produce oxaloacetate (OAA). The OAA is converted to malate by the reverse reaction of malate dehydrogenase and transported into the mitochondria to produce pyruvate and fumarate. The NADH formed during production of pyruvate from malate is used in the reduction of fumarate to succinate. The NADH-fumarate reductase system, which is the anaerobic electron transport system characteristic of adult *A. suum* mitochondria, is the final step of this pathway. Unique property of this pathway is discussed in the next section.

In contrast to larvae which require oxygen for their development and possess the respiratory system to be almost the same as that of mammals, cytochrome *c* oxidase (complex IV) is not found in the respiratory chain of adult *A. suum* mitochondria, and the content of ubiquinol–cytochrome *c* reductase complex (complex III) is extremely low [18]. In addition to the enzymes, quinone species in the mitochondria also change during the life cycle of *A. suum*. In contrast to adult mitochondria, in which the low-potential rhodoquinone (RQ; $Em' = -63mV$) is the major quinone, ubiquinone (UQ; $Em' = +110mV$) is the major quinone of larvae (Fig. 4A) [19]. A combination of SQR and UQ, and that of QFR and a low-potential quinone, such as RQ or menaquinone (MK), is also observed in *Escherichia coli* and other bacteria during metabolic adaptation to changes in

Please cite this article as: C. Sakai, et al., Mitochondrial fumarate reductase as a target of chemotherapy: From parasites to cancer cells, Biochim. Biophys. Acta (2012), doi:10.1016/j.bbagen.2011.12.013

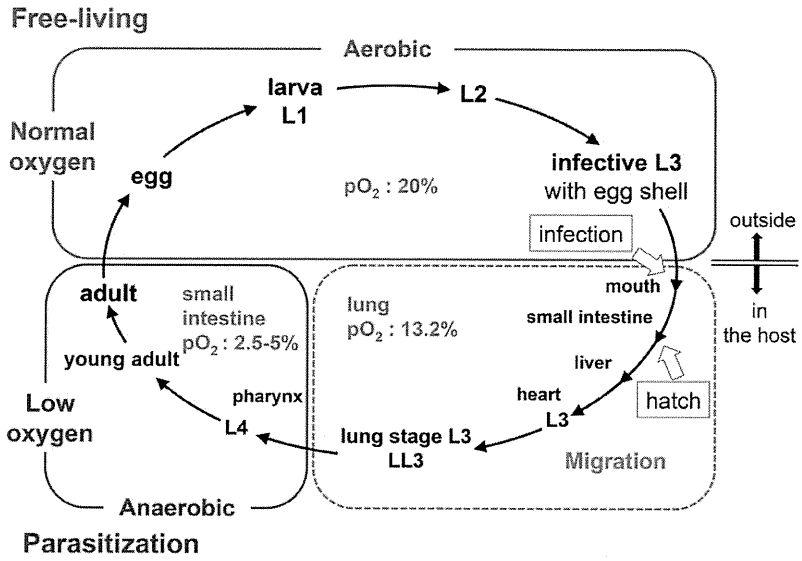

Fig. 2. Life cycle of *Ascaris suum*.Fertilized eggs grow to be infective L3 under aerobic environment. Infective L3 larvae are ingested by the host, reach the small intestine and hatch there. Afterwards, larvae migrate into host body (liver, heart, lung, pharynx), and finally migrate back to the small intestine and become adults. In the host small intestine, the oxygen concentration is low ($pO_2 = 2.5$~5%) compared with the exogenous environment ($pO_2 = 20\%$). The metabolic pathway of *A. suum* changes dramatically during its life cycle, to adapt to changes in the environmental oxygen concentration [6].

oxygen supply [20,21]. Lower potential of RQ and MK is favorable for the electron transfer from NADH to fumarate (Fig. 4B). In this way, UQ participates in aerobic metabolism in *A. suum* larva, whereas RQ participates in anaerobic metabolism in adult *A. suum*.

Although studies have shown a clear difference in energy metabolism between larval and adult *A. suum* mitochondria, little is known about changes in the properties of mitochondria during migration of *A. suum* larvae in the host. As described later, examination of the changes in enzymatic characteristics and subunit composition of *A. suum* larval complex II from lung stage L3 (LL3) larvae obtained from rabbits showed that properties of LL3 mitochondria differed from those of L3 and adult mitochondria [22]. Protein chemical analysis revealed that the change in complex II begins with the anchor subunit, and then occurs in the catalytic subunit. Thus, *A. suum* is able to adapt to changes in oxygen concentration in the environment during its life cycle by dynamic change of respiratory chain.

2.2. NADH-fumarate reductase system (fumarare respiration) of A. suum adult

The final step of the PEPCK–succinate pathway, which plays such an important role in the anaerobic energy metabolism of the *A. suum* adult, is catalyzed by the NADH-fumarate reductase system as

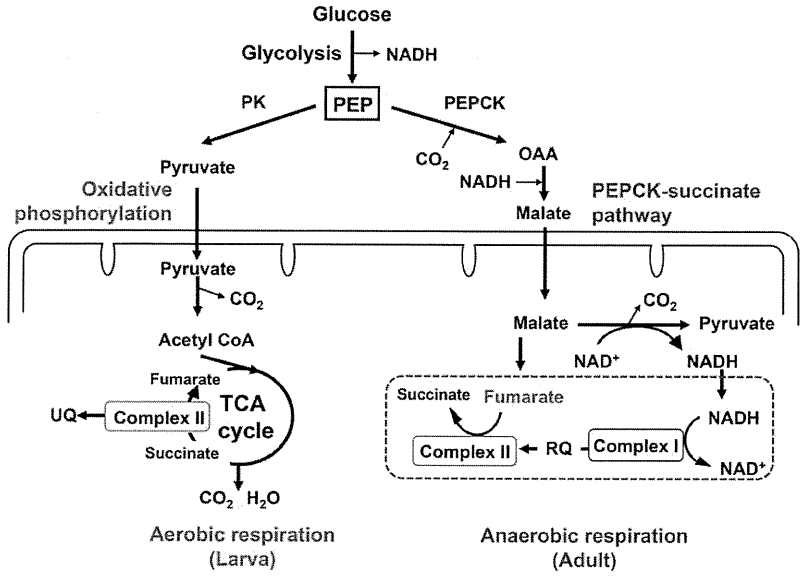

Fig. 3. Glucose metabolism of *A. suum* larval and adult mitochondria.The metabolic pathway of *A. suum* adult has a unique anaerobic electron transport system, NADH-fumarate reductase system. In the phospho*enol*pyruvate carboxykinase (PEPCK)–succinate pathway, phospho*enol*pyruvate (PEP) produced by a glycolytic process is carboxylated to form oxaloacetate and is then reduced to malate. The cytosolic malate is transported into the mitochondria, where it is first reduced to fumarate, and finally to succinate by the rhodoquinol–fumarate reductase activity of complex II. The terminal step is catalyzed by the NADH-fumarate reductase system (boxed in broken lines) comprised of complex I, rhodoquinone (RQ), and complex II. PEP, phosphoenolpyuvate; PEPCK, phoshoenolpyruvate carboxykinase; OAA, oxaloacete [6].

Please cite this article as: C. Sakai, et al., Mitochondrial fumarate reductase as a target of chemotherapy: From parasites to cancer cells, Biochim. Biophys. Acta (2012), doi:10.1016/j.bbagen.2011.12.013

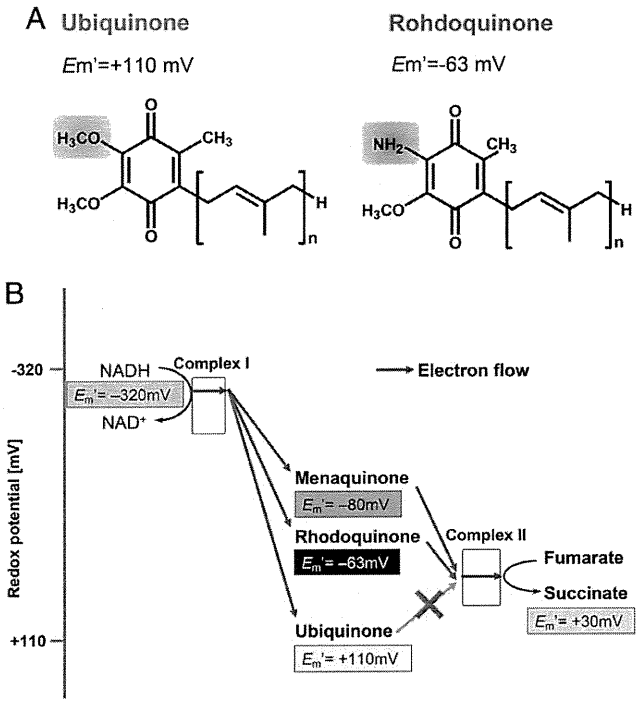

Fig. 4. Chemical structure and redox potentials of the quinones. A. Chemical structures of UQ and RQ. n, numbers of isoprenyl groups in side-chain. B. Redox potentials of quinones and substrates.

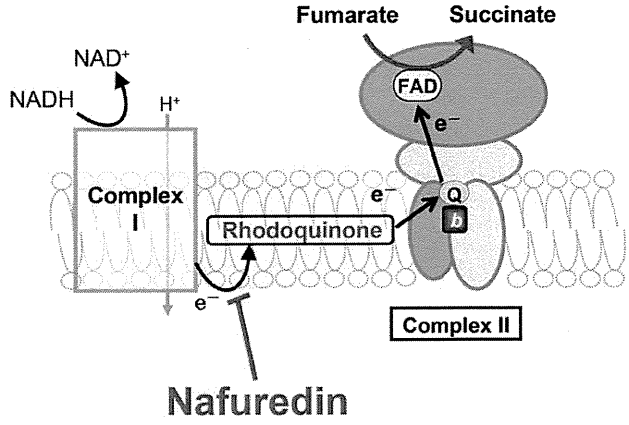

Fig. 5. NADH-fumarate reductase System of *A. suum* as a target of chemotherapy.The differences in energy metabolisms between host and helminths are an attractive therapeutic targets for helminthiasis. NADH-fumarate reductase is a part of a unique respiratory system in parasitic helminths and is the terminal step of the phospho*enol*pyruvate carboxykinase–succinate pathway, which is found in many anaerobic organisms. NADH-fumarate reductase system is a potential target for chemotherapy. Nafuredin was found to be competitive inhibitor for rhodoquinone binding site of *A. suum* complex II [1].

described in the previous section. This system is also called "fumarate respiration". The low-potential rhodoquinone transfers reducing equivalent of NADH via complex I to complex II, and finally succinate is produced by quinol fumarate reductase (QFR) activity of complex II. The merit of this system is to synthesize ATP using the coupling site of complex I even in the absence of oxygen, although its energy efficiency is low (Fig. 5).

A similar anaerobic respiration system exists in the mitochondria of many other parasites, and has also been found in bacteria. Extensive studies of bacteria, including *E. coli*, have revealed the details of this system [23,24]. In *E. coli*, there are two types of complex II, and QFR encoded by the *frd* operon is induced under anaerobic conditions. A low molecular weight mediator between complex I and complex II is menaquinone (MK; $Em' = -80$ mV), a low-potential naphthoquinone, in the *E. coli* fumarate respiration. In contrast, under aerobic conditions, SQR encoded by *sdh* operon that catalyzes oxidation of succinate is induced [25]. SQR is a dehydrogenase complex in the respiratory system as well as an enzyme in the TCA cycle, and directly connects these systems in aerobic energy metabolism.

Thus, two different enzymes (complex II) are present in *E. coli*, and the bacteria maintain homeostasis of the energy metabolism by controlling the synthesis of these enzymes in response to the environmental oxygen supply. How about the complex IIs of *A. suum*? Biochemical and molecular biological analyses showed *A. suum* also possesses two different complex IIs. However, subunit compositions and expression patterns are more complicated in the parasite complex II.

3. Complex IIs of *A. suum* mitochondria

3.1. Multiple complexes II in A. suum mitochondria

The complex II superfamily comprises succinate–quinone reductase (SQR) and quinol–fumarate reductase (QFR), which catalyze the interconversion of succinate and fumarate with quinone and quinol. SQR is a component of the aerobic respiratory chain as well as the tricarboxylic acid (TCA) cycle [26]. QFR is a component of the anaerobic respiratory chain in anaerobic and facultative anaerobic bacteria [27] and lower eukaryotes [6,28]. SQR and QFR complexes generally consist of four subunits referred to as the flavoprotein subunit (Fp), iron–sulfur subunit (Ip), cytochrome *b* large subunit (CybL), and cytochrome *b* small subunit (CybS). The Fp and Ip subunits comprise the catalytic domain of the enzyme. The Fp subunit has a FAD as a prosthetic group and contains the dicarboxylate-binding site. The Ip subunit generally contains three iron–sulfur clusters $[2Fe\text{–}2S]^{2+,1+}$, $[4Fe\text{–}4S]^{2+,1+}$, and $[3Fe\text{–}4S]^{1+,0}$. Subunits CybL and CybS, with heme *b* as the prosthetic group, form the anchor domain of the enzyme. This anchors the catalytic domain to the inner mitochondrial membrane and also serves as the quinone oxidation/reduction site [29].

Our previous study showed that *A. suum* mitochondria express stage-specific isoforms of complex II (SQR in larvae/QFR in adult) (Fig. 6). The Fp and CybS in adult complex II differ from those of infective third stage larval (L3) complex II. In contrast, there is no difference in the iron-sulfur cluster (Ip) and CybL between adult and L3 isoforms of complex II. However, recent analysis of the changes that occur in the respiratory chain of *A. suum* larvae during their migration in the host, we found that enzymatic activity, quinone content and complex II subunit composition in mitochondria of lung stage L3 (LL3) *A. suum* larvae is different from those of L3 and adult [22]. Quantitative analysis of quinone content in LL3 mitochondria showed that ubiquinone is more abundant than rhodoquinone. Interestingly, the results of two-dimensional bule-native/sodium dodecyl sulfate polyacrylamide gel electrophoresis analyses showed that LL3 mitochondria contained larval Fp (Fp^L) and adult Fp (Fp^A) at a ratio of 1:0.56, and that most LL3 CybS subunits were of the adult form ($CybS^A$). This result clearly indicates that the rearrangement of complex II begins with a change in the isoform of the anchor CybS subunit, followed by a similar change in the Fp subunit. At any event, the NADH-fumarate reductase activity of *A. suum* adult worms (~100 nmol/min/mg) are much higher than that of the mammalian host (2~5 nmol/min/mg).

3.2. ROS production from complex II

Mitochondrial respiratory chain is a significant source of cellular ROS. Impairment of the respiratory chain complexes is known to

Please cite this article as: C. Sakai, et al., Mitochondrial fumarate reductase as a target of chemotherapy: From parasites to cancer cells, Biochim. Biophys. Acta (2012), doi:10.1016/j.bbagen.2011.12.013

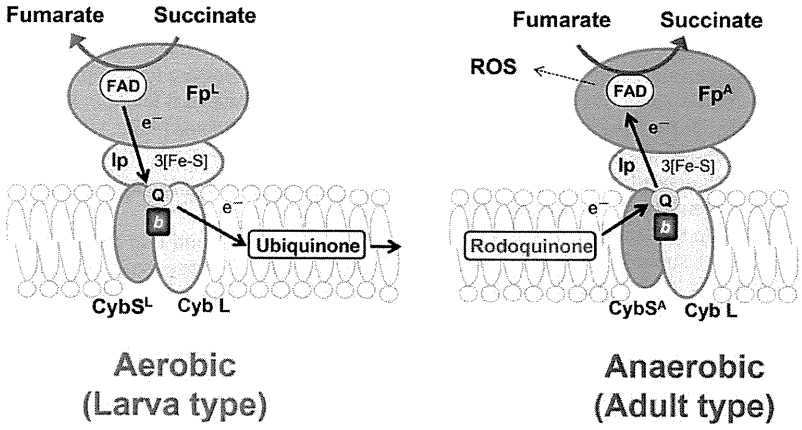

Fig. 6. Schematic representation of *A. suum* complexes II from larva type and adult type.The mitochondrial metabolic pathway of the parasitic nematode *A. suum* changes dramatically during its life cycle, to adapt to changes in the environmental oxygen concentration. *A. suum* mitochondria express stage-specific isoforms of complex II. While there is no difference in the isoforms of the Ip and cybL subunits of complex II between L3 larvae and adult A. *suum*, they have different isoforms of complex II subunits Fp (larval, Fp^L; adult, Fp^A) and cybS (larval, $cybS^L$; adult, $cybS^A$) in *A. suum* adult respiratory chain, complex II produces high amount ROS [29].

increase the cellular ROS production [30]. In general, complexes I and III are considered as the two major sites of superoxide and hydrogen peroxide production in the respiratory chain [30–33]. Interestingly, our results show that complex II is the main site of ROS production in *A. suum* adult respiratory chain [9].

Analysis of submitochondrial particles for superoxide ($O_2^{\cdot-}$) production using superoxide dismutase inhibitable acetylated cytochrome *c* reduction, and hydrogen peroxide production using catalase inhibitable amplex red oxidation, in the presence and absence of respiratory chain inhibitors, showed the contribution from both the FAD site and quinone-binding site of complex II to produce $O_2^{\cdot-}$ and H_2O_2 when succinate is oxidized under aerobic conditions. Considering the conservation of amino acid residues critical for the enzyme reaction between *A. suum* complex II and mitochondrial SQR, our results show the ROS production from more than one site in mitochondrial complex II linked with subtle differences in the amino acid sequences of the enzyme complex.

A. suum adult complex II is a good model to study the mechanism of ROS production from mitochondrial complex II, since amino acid residues conserved among the catalytic domains in mitochondrial SQR enzymes are well conserved in this enzyme and it produces high levels of ROS. Absence of complex III and IV activities in its respiratory chain is an additional advantage of this model. These studies will provide further insight into the possibility of high levels of ROS production from both the FAD site and the Q site in the complex II of *A. suum* adult worm and help to understand the role of mutations in human complex II for carcinogenesis.

3.3. Specific inhibitors of complex II

The differences between parasite and host mitochondria described in this review hold great promise as targets for chemotherapy. For example, the anti-malarial drug Atovaquone, which was recently developed, acts on the mitochondrial respiratory chain [34]. Atovaquone is effective against chloroquine-resistant strains, [35]. The specific target is thought to be complex III, and biochemical analysis has shown that it acts on the ubiquinone oxidation site in the cytochrome *b* of complex III [36,37]. Such a chemotherapeutic approach is also applicable to the helminthes. It has been proposed that the fumarate respiration is the target of such drugs as bithionol and thiabendazole [38,39], but there is no clear biochemical or pharmaceutical evidence to support this idea. However, as described in the previous section, progress in the study of the NADH-fumarate reductase pathway permits screening of new anthelmintic compound. Nafuredin, selectively inhibits helminth complex I at concentrations in the order of nanomoles [40] (Fig. 7). Kinetic analysis revealed that the inhibition by nafuredin is competitive against RQ (Fig. 5). These findings, coupled with the fact that helminth complex I uses both RQ and UQ as an electron acceptor, suggest that the structural features of the quinone reduction site of helminth complex I may differ from that of mammalian complex I. In fact, the inhibitory mechanism of quinazolines, which effectively kill the *E. multilocularis* protoscoleces, was competitive and partially competitive against RQ and UQ, respectively [41].

The most potent inhibitor of complex II, Atpenin A5, was found during the screening of inhibitors for *A. suum* complex II [42]. To our regret, IC_{50} of Atpenin A5 for bovine complex II (3.6 nM) was lower than that for *A. suum* complex II (12 nM for QFR and 32 nM for SQR). However, further screening of inhibitors showed that flutolanil, a commercially available fungicide, specifically inhibits *A. suum* SQR [43] (Fig. 7). The IC_{50} of flutolanil against *A. suum* and bovine SQR was 0.081 and 16 μM, respectively, indicating that flutolanil is a promising lead compound for anthelminthics. To enable rational drug optimization, a crystal of the *A. suum* QFR complexed with

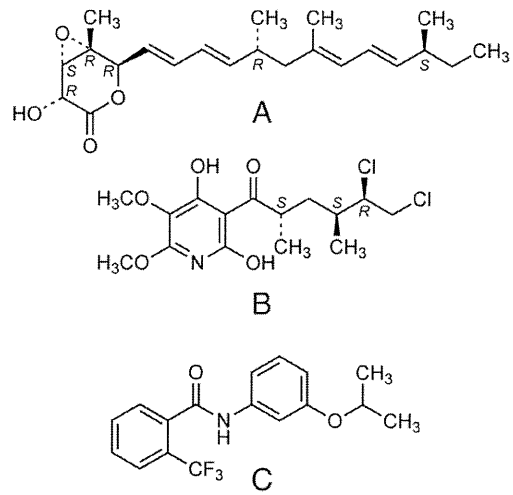

Fig. 7. Chemical structure of inhibitors of complex II.A. Nafuresin, a competitive inhibitor for the rhodoquinone binding site of *A. suum* complex II; B. Atpenin A5, a competitive inhibitor for the quinone binding site of complex II of many species; C. Fulutolanil, a competitive inhibitor for the quinone binding site of *A. siuum* complex II.

Please cite this article as: C. Sakai, et al., Mitochondrial fumarate reductase as a target of chemotherapy: From parasites to cancer cells, Biochim. Biophys. Acta (2012), doi:10.1016/j.bbagen.2011.12.013

flutolanil was prepared by soaking, and X-ray structure analysis has been performed. The current structural model of the flutolanil bound form of the *A. suum* QFR (Harada, unpublished observation) indicates that flutolanil is bound to the same site as those of the quinone binding observed in complex IIs from pig heart mitochondria (pdb code 1ZOY), *E. coli* (1NEK and 1L0V) and avian (1YQ4). The site of the pig enzyme, for example, is composed of ten residues highly conserved across amino acid sequences of these complex IIs; Pro169, Trp173 and Ile218 from the Ip subunit, Ile30, Trp35, Met39, Ser42, Ile43 and Arg46 from the CybL subunit, and Tyr91 from the CybS subunit. However, three residues, Trp35, Met39 and Ile53, are replaced by Pro65, Trp69 and Gly73, respectively, in *A. suum* QFR. The structures of the *A. suum* QFR together with those of QFRs from *Wolinella succinogenes* [24] and *E. coli* [23], and SQRs from *E. coli* [44], pig heart mitochondria [45], and avian heart mitochondria [46] should help clarify the structure–function relationship of complex II and provide useful information for the structure-based design of anthelminthics.

4. Fumarate respiration of human mitochondria

4.1. Human complex II

In human, many cases of diseases caused by mutations in subunits of complex II have been reported. Mutations found in the Ip, Cyb L or Cyb S are associated with the development of pheochromocytoma and paraganglioma [47–51]. It is suggested that the causes of tumorigenesis are ROS production from mutated complex II [52,53] or accumulation of succinate as a result of SQR inhibition [11]. Accumulated succinate inhibits HIF-1α prolyl hydroxylases in the cytosol, leading to stabilization and activation of HIF-1α. Thus, succinate can increase expression of genes that facilitate angiogenesis, metastasis, and glycolysis, ultimately leading to tumor progression. On the other hand, no patient with mutation in Fp linked to tumorigenesis has been reported. There are two Fp isoforms in human, which will be discussed later, and this is probably the reason why mutations in Fp are not directly linked to tumorigenesis. Instead, mutations in Fp are linked to severe metabolic disorders resulting from decreased activity of the TCA cycle and impairment of oxidative phosphorylation, although these are rare. These autosome-recessive disorders are manifested as childhood encephalopathy, myopathy, adult optic atrophy, and Leigh syndrome [54–57]. Recently, two new proteins, SDHAF1 (succinate dehydrogenase complex assembly factor 1) and SDHAF2, were found to be the first assembly factors of complex II [53,58]. It was suggested that mutations found in SDHAF1 may result in the reduction of assembled complex II and cause infantile leukoencephalopathy [58]. SDHAF2 is suggested to be required for the incorporation of the flavin adenine dinucleotide cofactor (flavination) of SDHA (succinate dehydrogenase complex, subunit A, flavoprotein), and it is also necessary for complex II assembly and function [53]. Furthermore, the mutation found in SDHAF2 has been suggested to link to familial paraganglioma [53]

4.2. Isoforms of human complex II

In 2003, we found two isoforms of human Fp, type I and type II [59,60] (Fig. 8). These isoforms differ from each other only in two amino acid residues. Tyr 586 and Val 614 of type I Fp are replaced by Phe 586 and Ile 614 in type II Fp, respectively. Tyr 586 and Val 614 are well conserved among mammals' Fps and type II Fp is found only in human complex II (Fig. 9). Type I Fp gene has an exon–intron structure, while the structure of type II Fp gene has not been determined. The type II Fp gene is not found in the NCBI database and the location has not been clarified yet while type I Fp gene is located on chromosome 5p15 [59,60].

Complex II with type I Fp has isoelectric point (p*I*) of 6–7, whereas complex II with type II Fp shows its p*I* of 5–6. To explain the difference of p*I* values, several reports suggested the phosphorylation of amino acid residues in Fp subunit [7,61]. One of these residues, Tyr 500, is located close to Tyr 586, which is replaced by Phe in type II Fp (Fig. 10). Since the Tyr 586 Phe substitution will certainly destroy a hydrogen bond between Tyr 586 O_η and Glu 597 O_δ (3.13Å), the local structure around Tyr 586 as well as Tyr 500 phosphorylation status may be different between Fps of types I and II.

The result of biochemical analysis of complex II with each isoform, complex II with each Fp was found to have almost the same SQR specific activities. However, type II Fp has lower optimal pH than type I Fp and at optimal pH of type II Fp, K_m value for succinate of type II Fp is lower than type I Fp (Sakai unpublished data). It may be possible that different phosphorylation statuses of complex II with each isoform cause biochemical differences.

4.3. Expression of human complex II containing type II Fp

Our previous study on the expression of isoforms showed that both types were expressed in all the organs tested (liver, heart, skeletal muscle, brain and kidney) and expression of type I Fp was higher than that of type II Fp [59,60]. This tendency was also found in the cultured cells such as Fibroblast, Myoblast, Human Umbilical Vein Endothelial Cells (HUV-EC-C), colon cancer cells (HT-29) and lung cancer cells (A549). However, colorectal adenocarcinoma cells (DLD-1), breast cancer cells (MCF-7) and lymphoma cells (Raji) showed higher expression of type II than that of type I Fp. Type I Fp seems to be essential for the ordinary function of complex II because

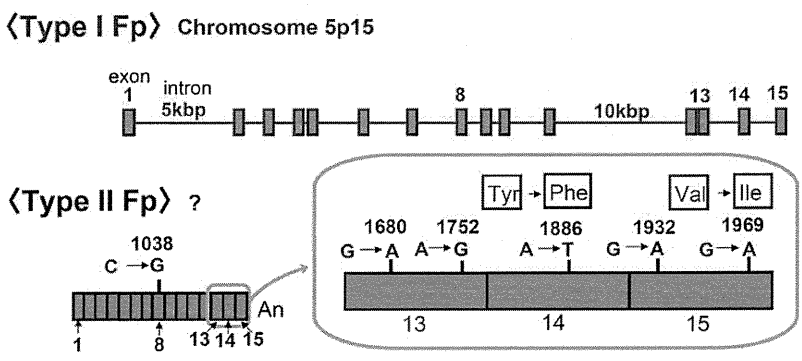

Fig. 8. Fp isoform gene structure.Type I and II Fps differ from each other in six bases in DNA sequences and in two amino acid residues in proteins. Type I Fp gene has an exon–intron structure, while type II Fp gene issuggested to be intron-less. Although type I Fp gene is located on chromosome 5p15, the type II Fp gene is not found in the NCBI database and the location has not been clarified yet [59,60].

Please cite this article as: C. Sakai, et al., Mitochondrial fumarate reductase as a target of chemotherapy: From parasites to cancer cells, Biochim. Biophys. Acta (2012), doi:10.1016/j.bbagen.2011.12.013

```
Human type I Fp  578 HWRKHTLSYVDVGTGKVTLEYRPVI DKTLNEADCATVPPAI RSY
Human type II Fp 578 HWRKHTLSFVDVGTGKVTLEYRPVI DKTLNEADCATIPPAI RSY
Rat Fp           570 HWRKHTLSYVDTKTGKVTLDYRPVI DKTLNEADCATVPPAI RSY
Mouse Fp         578 HWRKHTLSYVDI KTGKVTLEYRPVI DKTLNEADCATVPPAI RSY
Bovine Fp        582 HWRKHTLSYVDI KTGKVTLEYRPVI DRTLNETDCATVPPAI GSY
                         Y586F                   V614I
```

Fig. 9. Alignment of amino acid sequences of Mammalian Fp subunits.Two amino acid residues in the red box are different in human Fp isoforms. Tyr 586 and Val 614 in type I Fp are changed to Phe 586 and Ile 614 in type II Fp, respectively. Tyr 586 and Val 614 are well conserved among mammals and no animals but humans have type II Fp [59].

all the examined tissues and many of the cultured cells showed abundant expression of type I Fp and optimum pH for this isoform is around physiological mitochondrial matrix pH (pH8.0).

Since type II Fp was expressed in some cancer cells, this isoform may play an important role in the metabolism of tumor tissue. To investigate the link between type II Fp and tumor tissue in detail, we analyzed mRNA expression ratio of Fp isoforms in several tissues including tumor tissues and cultured cells. Since some tumor marker genes are expressed in fetal tissues, we included the fetal tissues in this analysis.

As shown in Table 1, in cultured cells, all the normal cells tested showed mainly type I Fp expression as reported previously [59,60]. In tissues, expression of type I Fp was higher than that of type II Fp in all the organs tested including normal testes tissue. Interestingly, normal pancreatic tissue showed higher expression of type II Fp. In addition, several tumor tissues expressed predominantly type II Fp such as breast tumor, liver tumor, kidney tumor and cervix tumor. Among fetal tissues, brain and skeletal muscle showed higher expression of type II Fp than type I Fp.

4.4. Fumarate respiration of human cancer cells

Several observations suggested the presence of a reverse reaction of complex II, fumarate reductase (FRD), in mammalian cells, although no direct evidence of FRD activity in mammalian complex II has been available until recently [62,63]. The accumulation of succinate under hypoxic conditions has been reported, and complex II has been suggested to function as FRD in mammalian cells [64]. Metabolome analysis of the cancer cells supports this idea, because succinate, fumarate and malate were present at higher levels in cancer tissues than normal tissues [65]. FRD inhibitor pyrvinium pamoate, an anthelmintic, has also been reported to act as an anticancer compound in human cancer cells [62]. Furthermore, recent biochemical studies showed fumarate respiration in human mitochondria clearly [7,8]. Mitochondria isolated from DLD-1 cells showed FRD activity with 3 nmol/min/mg protein, although this number is quite lower than that of the *A. suum* mitochondria (200 nmol/min/mg). Interestingly, the cancer cells had higher FRD/SQR ratio than the normal cells. For example, FRD/SQR ratio in Panc-1 cells is 0.066 ± 0.010, while that in Human Dermal Fibroblast cells is 0.011 ± 0.002. In addition, FRD/SQR ratio increased when the cancer cells were cultured under hypoxic and glucose limited condition [7]. Effect of a treatment by phosphatase and protein kinase on the direction of enzyme activity of human complex II suggests the changes from SQR to QFR by phosphorylation of Fp.

Different from *A. suum*, which has at least two distinct complex IIs as mentioned previously, only one gene is found for each subunit of human complex II except Fp. In this connection, it is of interest to speculate that complex II with type II Fp has higher QFR activity and plays an important role in fumarate respiration in human mitochondria as terminal oxidase of the system. Further biochemical study on

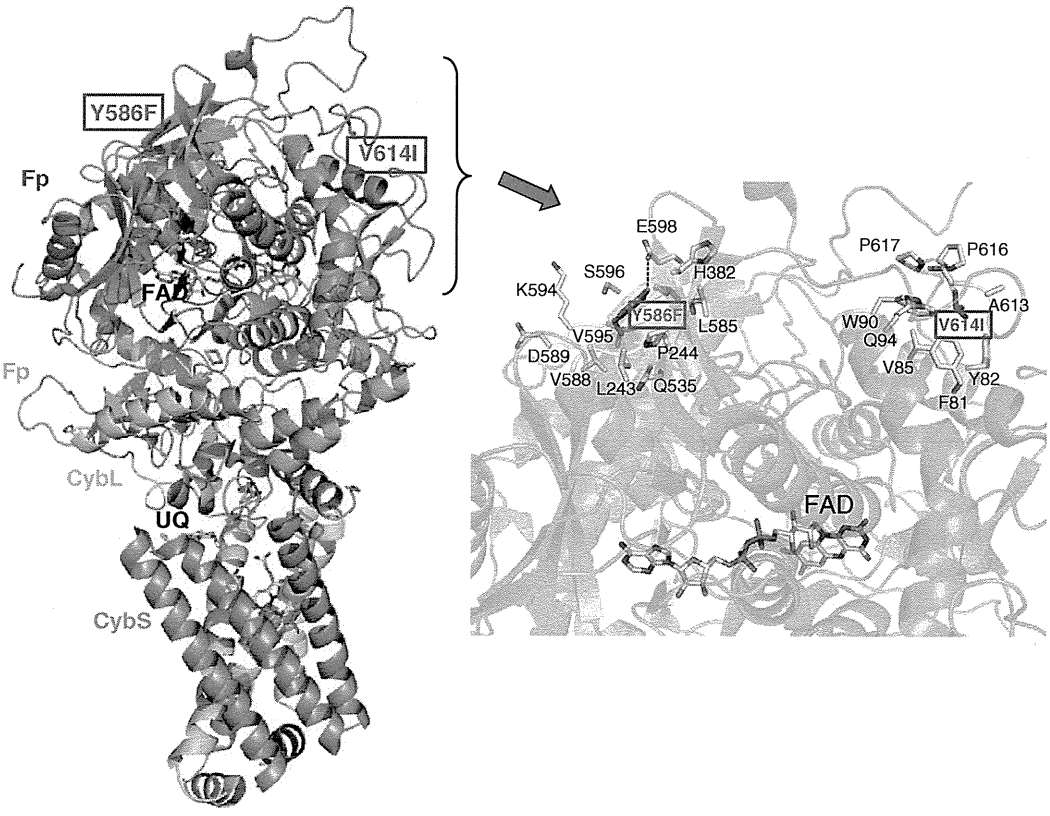

Fig. 10. Positions of Tyr 586 and Val 614 in the structure of porcine complex II.Two amino acid residues different in human isoforms, Y586F and V614I, shown in the cartoon representation of the porcine complex II structure (left) and the close-up view of the region including Y586F and V614I (right). V614I is surrounded mainly by hydrophobic residues, whereas Y586F by both hydrophilic and hydrophobic residues. Y586 and E598 are in the hydrogen bond distance (3.15 Å) to each other. UQ shows ubiquinone. The numbers of amino acid residues in the box represent the human amino acid sequences and the others are the porcine amino acid sequences.

Please cite this article as: C. Sakai, et al., Mitochondrial fumarate reductase as a target of chemotherapy: From parasites to cancer cells, Biochim. Biophys. Acta (2012), doi:10.1016/j.bbagen.2011.12.013

Table 1
mRNA expression of Fp isoforms in human cultured cells and tissues.

The expression ratio of the two Fp isoforms was analyzed by RT-PCR-RFLP (restriction fragment length polymorphism with AvaII). Total RNAs were obtained from NIPPON GENE (Japan) for normal liver, heart, skeletal muscle, brain, kidney and breast tumor, colon tumor, stomach tumor and uterus tumor. Wako (Japan) for normal pancreas and fetal tissues. Invitrogen (USA) for normal testes and breast tumor, liver tumor, kidney tumor, colon tumor, pancreas tumor, cervix tumor, ovary tumor, prostate tumor. Cells; Fibroblast and Myoblast: kind gift from Dr. Yu-ichi Goto (National Institute of Neuroscience, Japan) A549, DLD-1 and MCF-7: kind gift from Mr. Yasuyuki Yamazaki (Taiho pharma ceutical, Japan) Panc-1: kind gift from Dr. Yasuhiro Esumi (National Cancer Institute, Japan) Raji: kind gift from Dr. Kazurou Shiomi (Kitasato university, Japan) HT-29, HU-VEC-C, MDA-M-231, BT-20 and T-47D: ATCC (USA). Pancreatic epithelial and stromal cells: DS pharma (Japan).

		Race	Gender	Age	I (%)/II (%)
Tissue (normal)	Liver*	Caucasoid	Female	15	70/30
	Heart*	Caucasoid	Pool of 7 donors		61/39
	Skeletal muscle*	—	Male	23	80/20
	Brain*	Caucasoid	Male	50	84/16
	Kidney*	Caucasoid	Pool of 8 donors		62/38
	Pancreas	—	Male	44	30/70
	Testes	Caucasoid	Male	19	100/0
Cell (normal)	Fibroblast*	Mongoloid	—	—	94/6
	Myoblast*	Mongoloid	—	—	87/13
	HUV-EC-C*	—	—	—	88/12
	Pancreatic epithelial	—	—	—	100/0
	Pancreatic stromal	—	—	—	100/0
Tissue (fetal)	Brain	—	Female	22 weeks	100/0
	Brain	—	Male	41 weeks	38/62
	Skeletal muscle	—	Male	22 weeks	0/100
	Skeletal muscle	—	Female	19 weeks	100/0
Tissue (cancer)	Breast	—	Female	55	100/0
	Breast	Mongoloid	Female	Pool of 6 donors	0/100
	Liver	Caucasoid	Male	60	0/100
	Kidney	Caucasioid	Female	54	23/77
	Colon	Caucasoid	Male	75	100/0
	Colon	—	—	—	100/0
	Pancreas	Mongoloid	Male	32	100/0
	Stomach	—	—	—	100/0
	Uterus	—	Female	—	100/0
	Cervix	Caucasoid	Female	59	23/77
	Ovary	Caucasoid	Female	32	100/0
	Prostate	—	Male	—	100/0
Cell (cancer)	HT29*	Caucasoid	Female	44	92/8
	A549*	Caucasoid	Male	58	96/4
	DLD-1*	—	Male	—	25/75
	MCF-7*	Caucasoid	Female	69	23/77
	Raji*	Neglod	Male	11	17/83
	Panc-1	Caucasoid	Male	56	12/88
	MDA-M-231	Caucasoid	Female	51	100/0
	BT-20	Caucasoid	Female	78	78/22
	T-47D	Caucasoid	Female	54	53/47

* Tomitsuka, et al. [59,60].

the difference between type I and type II Fp will bring final conclusion on this attractive idea.

5. Conclusions

The recent findings described in this review indicate that the respiratory chain plays an important role in responses to changes in the amount of oxygen in the environment. Complex II functions as a fumarate reductase during adaptation to a hypoxic condition to ensure the maintenance of oxygen homeostasis. In this connection, the reports indicating that complex II functions as an oxygen sensor are of great interest [63].

In addition, direct evidence of fumarate respiration in human mitochondria are quite important in the study of energy metabolism in hypoxic condition including cancer cells. Differences in energy metabolism between hosts and parasites and/or cancer cells are attractive therapeutic targets.

Acknowledgements

This work was supported in part by Creative Scientific Research Grant 18GS0314 (to KK), Grant-in-aid for Scientific Research on Priority Areas 18073004 (to KK) from the Japanese Society for the Promotion of Science, and Targeted Proteins Research Program (to KK) from the Japanese Ministry of Education, Science, Culture, Sports and Technology (MEXT).

References

[1] K. Kita, K. Shiomi, S. Ōmura, Parasitology in Japan: advances in drug discovery and biochemical studies, Trends Parasitol. 23 (2007) 223–229.
[2] A. Kroger, V. Geisler, E. Lemma, F. Theis, R. Lenger, Bacterial fumarate respiration, Arch. Microbiol. 158 (1992) 311–314.
[3] T. Kuramochi, H. Hirawake, S. Kojima, S. Takamiya, R. Furushima, T. Aoki, R. Komuniecki, K. Kita, Sequence comparison between the flavoprotein subunit of the fumarate reductase (complex II) of the anaerobic parasitic nematode, *Ascaris suum* and the succinate dehydrogenase of theaerobic, free-living nematode, *Caenorhabditis elegans*, Mol. Biochem. Parasitol. 68 (1994) 177–187.
[4] F. Saruta, H. Hirawake, S. Takamiya, Y.-C. Ma, T. Aoki, K. Sekimizu, S. Kojima, K. Kita, Cloning of a cDNA encoding the small subunit of cytochrome b_{558} (cybS) of mitochondrial fumarate reductase (complex II) from adult *Ascaris suum*, Biochim. Biophys. Acta 1276 (1996) 1–5.
[5] H. Amino, H. Wang, H. Hirawake, F. Saruta, D. Mizuchi, R. Mineki, N. Shindo, K. Murayama, S. Takamiya, T. Aoki, S. Kojima, K. Kita, Stage-specific isoforms of *Ascaris suum* complex II: the fumarate reductase of the parasitic adult and the succinate dehydrogenase of free-living larvae share a common iron-sulfur subunit, Mol. Biochem. Parasitol. 106 (2000) 63–76.
[6] K. Kita, S. Takamiya, Electron-transfer complexes in *Ascaris* mitochondria, Adv. Parasitol. 51 (2002) 95–131.
[7] E. Tomitsuka, K. Kita, H. Esumi, Regulation of succinate–ubiquinone reductase and fumarate reductase activities in human complex II by phosphorylation of its flavoprotein subunit, Proc. Jpn. Acad. Ser. B Phys. Biol. Sci. 85 (2009) 258–265.
[8] E. Tomitsuka, K. Kita, H. Esumi, The NADH-fumarate reductase system, a novel mitochondrial energy metabolism, is a new target for anticancer therapy in tumor microenvironments, Ann. N. Y. Acad. Sci. 201 (2011) 44–49.
[9] M.P. Paranagama, K. Sakamoto, H. Amino, M. Awano, H. Miyoshi, K. Kita, Contribution of the FAD and quinone binding sites to the production of reactive oxygen species from *Ascaris suum* mitochondrial complex II, Mitochondrion 10 (2010) 158–165.
[10] R.D. Guzy, B. Sharma, E. Bell, N.S. Chandel, P.T. Schumacker, Loss of the SdhB, but Not the SdhA, subunit of complex II triggers reactive oxygen species-dependent hypoxia-inducible factor activation and tumorigenesis, Mol. Cell. Biol. 28 (2008) 718–731.
[11] M.A. Selak, S.M. MacKenzie, H. Boulahbel, D.G. Watson, K.D. Mansfield, Y. Pan, M.C. Simon, C.B. Thompson, E. Gottlieb, Succinate links TCA cycle dysfunction to oncogenesis by inhibiting HIF-alpha prolyl hydroxylase, Cancer Cell 7 (2005) 77–85.
[12] R. Komuniecki, B.G. Harris, J. Marr, M. Mueller, Biochemistry and Molecular Biology of Parasites, Academic Press, London, 1995, pp. 49–66.
[13] A.G.M. Tielens, J. Van Hellemond, The electron transport chain in anaerobically functioning eukaryotes, Biochim. Biophys. Acta 1365 (1998) 71–78.
[14] K. Kita, H. Hirawake, S. Takamiya, Cytochromes in the respiratory chain of helminth mitochondria, Int. J. Parasitol. 27 (1997) 617–630.
[15] J. Matsumoto, K. Sakamoto, N. Shinjyo, Y. Kido, N. Yamamoto, K. Yagi, H. Miyoshi, N. Nonaka, K. Katakura, K. Kita, Y. Oku, Anaerobic NADH-fumarate reductase system is predominant in the respiratory chain of *Echinococcus multilocularis*, providing a novel target for the chemotherapy of alveolar echinococcosis, Antimicrob. Agents Chemother. 52 (2008) 164–170.
[16] P. Kohler, R. Bachmann, Mechanisms of respiration and phosphorylation in *Ascaris* muscle mitochondria, Mol. Biochem. Parasitol. 1 (1980) 75–90.
[17] H. Oya, K. Kita, in: E. Bennet, C. Behm, C. Bryant (Eds.), Comparative Biochemistry of Parasitic Helminths, Chapman and Hall, London, 1988, pp. 35–53.
[18] S. Takamiya, R. Furushima, R.H. Oya, Electron transfer complexes of *Ascaris suum* muscle mitochondria: I. Characterization of NADH-cytochrome *c* reductase (complex I–III), with special reference to cytochrome localization, Mol. Biochem. Parasitol. 13 (1984) 121–134.
[19] S. Takamiya, K. Kita, H. Wang, P.P. Weinstein, A. Hiraishi, H. Oya, T. Aoki Developmental, Changes in the respiratory chain of *Ascaris* mitochondria, Biochim. Biophys. Acta 1141 (1993) 65–74.
[20] S.T. Cole, C. Condon, B.D. Lemire, J.H. Weiner, Molecular biology, biochemistry and bioenergetics of fumarate reductase, a complex membrane-bound iron–sulfur flavoenzyme of *Escherichia coli*, Biochim. Biophys. Acta 811 (1985) 381–403.
[21] A. Hiraishi, Fumarate reduction systems in members of the family *Rhodospirillaceae* with different quinone types, Arch. Microbiol. 150 (1988) 56–60.
[22] F. Iwata, N. Shinjyo, H. Amino, K. Sakamoto, M.K. Islam, N. Tsuji, K. Kita, Change of subunit composition of mitochondrial complex II (succinate–ubiquinone reductase/quinol–fumarate reductase) in *Ascaris suum* during the migration in the experimental host, Parasitol. Int. 57 (2008) 54–61.

Please cite this article as: C. Sakai, et al., Mitochondrial fumarate reductase as a target of chemotherapy: From parasites to cancer cells, Biochim. Biophys. Acta (2012), doi:10.1016/j.bbagen.2011.12.013

[23] T.M. Iverson, C. Luna-Chavez, G. Cecchini, D.C. Rees, Structure of the *Escherichia coli* fumarate reductase respiratory complex, Science 284 (1999) 1961–1966.
[24] C.R. Lancaster, A. Kröger, M. Auer, H. Michel, Structure of fumarate reductase from *Wolinella succinogenes* at 2.2 A resolution, Nature 402 (1999) 377–385.
[25] K. Kita, C. Vibat, S. Meinhardt, J. Guest, R. Gennis, One-step purification from *Escherichia coli* of complex II (succinate: ubiquinone oxidoreductase) associated with succinate-reducible cytochrome b_{556}, J. Biol. Chem. 264 (1989) 2672–2677.
[26] G. Cecchini, I. Schroder, R.P. Gunsalus, E. Maklashina, Succinate dehydrogenase and fumarate reductase from *Escherichia coli*, Biochim. Biophys. Acta 1553 (2002) 140–157.
[27] C.R.D. Lancaster, Structure and function of succinate: quinone oxidoreductases and the role of quinol: fumarate reductases in fumarate respiration, in: D. Zannoni (Ed.), Respiration in Archaea and Bacteria: Diversity of Prokaryotic Electron Transport Carriers, Kluwer Academic Publishers, The Netherlands, 2004, pp. 57–85.
[28] J.J. Van Hellmond, A. van der Klei, S.W.H. van Weelden, A.G.M. Tielens, Biochemical and evolutionary aspects of anaerobically functioning bacteria, Philos. Trans. R. Soc. B 358 (2003) 205–215.
[29] K. Kita, H. Hirawake, H. Miyadera, H. Amino, S. Takeo, Role of complex II in anaerobic respiration of the parasite mitochondria from *Ascaris suum* and *Plasmodium falciparum*, Biochim. Biophys. Acta 1553 (2002) 123–139.
[30] H.P. Indo, M. Davidson, H.C. Yen, S. Suenaga, K. Tomita, T. Nishii, M. Higuchi, Y. Koga, T. Ozawa, H.J. Majima, Evidence of ROS generation by mitochondria in cells with impaired electron transport chain and mitochondrial DNA damage, Mitochondrion 7 (2007) 106–118.
[31] P. Jezek, L. Hlavata, Mitochondria in homeostasis of reactive oxygen species in cell, tissues, and organism, Int. J. Biochem. Cell Biol. 37 (2005) 2478–2503.
[32] M.P. Murphy, How mitochondria produce reactive oxygen species, Biochem. J. 417 (2009) 1–13.
[33] J. St-Pierre, J.A. Buckingham, S.J. Roebuck, M.D. Brand, Topology of superoxide production from different sites in the mitochondrial electron transport chain, J. Biol. Chem. 277 (2002) 44784–44790.
[34] I.K. Srivastava, H. Rottenberg, A.B. Vaidya, Atovaquone, a broad spectrum antiparasitic drug, collapses mitochondrial membrane potential in a malarial parasite, J. Biol. Chem. 272 (1997) 3961–3966.
[35] S. Looareesuwan, C. Viravan, H.K. Webster, D.E. Kyle, D.B. Hutchinson, C.J. Canc eld, Clinical studies of atovaquone, alone or in combination with other antimalarial drugs, for treatment of acute uncomplicated malaria in Thailand, Am. J. Trop. Med. Hyg. 54 (1996) 62–66.
[36] D. Syafruddin, J.E. Siregar, S. Marzuki, Mutations in the cytochrome *b* gene of *Plasmodium berghei* conferring resistance to atovaquone, Mol. Biochem. Parasitol. 104 (1999) 185–194.
[37] I.K. Srivastava, J.M. Morrisey, E. Darrouzet, F. Daldal, A.B. Vaidya, Resistance mutations reveal the atovaquone-binding domain of cytochrome *b* in malaria parasites, Mol. Microbiol. 33 (1999) 704–711.
[38] P. Kohler, R. Bachmann, The effects of the antiparasitic drugs levamisole, thiabendazole, praziquantel, and chloroquine on mitochondrial electron transport in muscle tissue from *Ascaris suum*, Mol. Biochem. Parasitol. 14 (1978) 155–163.
[39] A. Armson, W.B. Grubb, A.H.W. Mendis, The effect of electron transport (ET) inhibitors and thiabendazole on the fumarate reductase (FR) and succinate dehydrogenase (SDH) of *Strongyloides ratti* infective (L3) larvae, Int. J. Parasitol. 25 (1995) 261–263.
[40] S. Omura, H. Miyadera, H. Ui, K. Shiomi, Y. Yamaguchi, R. Masuma, T. Nagamitsu, D. Takano, T. Sunazuka, A. Harder, H. Kölbl, M. Namikoshi, H. Miyoshi, K. Sakamoto, K. Kita, An anthelmintic compound, nafuredin, shows selective inhibition of complex I in helminth mitochondria, Proc. Natl. Acad. Sci. U. S. A. 98 (2001) 60–62.
[41] T. Yamashita, T. Ino, H. Miyoshi, K. Sakamoto, A. Osanai, E. Nakamaru-Ogiso, K. Kita, Rhodoquinone reaction site of mitochondrial complex I, in parasitic helminth, *Ascaris suum*, Biochim. Biophys. Acta 1608 (2004) 97–103.
[42] H. Miyadera, K. Shiomi, H. Ui, Y. Yamaguchi, R. Masuma, H. Tomoda, H. Miyoshi, A. Osanai, K. Kita, S. Omura, Atpenins, potent and specific inhibitors of mitochondrial complex II (succinate-ubiquinone oxidoreductase), Proc. Natl. Acad. Sci. U. S. A. 100 (2003) 473–477.
[43] A. Osanai, S. Harada, K. Sakamoto, H. Shimizu, D.K. Inaoka, K. Kita, Crystallization of mitochondrial rhodoquinol–fumarate reductase from the parasitic nematode *Ascaris suum* with the specific inhibitor flutolanil, Acta Crystallogr. Sect. F Struct. Biol. Cryst. Commun. 65 (2009) 941–954.
[44] V. Yankovskaya, R. Horsefield, S. Törnroth, C. Luna-Chavez, H. Miyoshi, C. Léger, B. Byrne, G. Cecchini, S. Iwata, Architecture of succinate dehydrogenase and reactive oxygen species generation, Science 299 (2003) 700–704.
[45] F. Sun, X. Huo, Y. Zhai, A. Wang, J. Xu, D. Su, M. Bartlam, Z. Rao, Crystal structure of mitochondrial respiratory membrane protein complex II, Cell 121 (2005) 1043–1057.
[46] L.S. Huang, G. Sun, D. Cobessi, A.C. Wang, J.T. Shen, E.Y. Tung, V.E. Anderson, E.A. Berry, 3-nitropropionic acid is a suicide inhibitor of mitochondrial respiration that, upon oxidation by complex II, forms a covalent adduct with a catalytic base arginine in the active site of the enzyme, J. Biol. Chem. 281 (2006) 5965–5972.
[47] J.P. Bayley, P. Devilee, E.M.P. Taschner, The SDH mutation database: an online resource for succinate dehydrogenase sequence variants involved in pheochromocytoma, paraganglioma and mitochondrial complex II deficiency, BMC Med. Genet. 6 (2005) 39.
[48] B.E. Baysal, On the association of succinate dehydrogenase mutations with hereditary paraganglioma, Trends Endocrinol. Metab. 14 (2003) 453–459.
[49] C. Eng, M. Kiuru, M.J. Fernandez, L.A. Aaltonen, A role for hypoxic mitochondrial enzymes in inherited neoplasia and beyond, Nat. Rev. Cancer 3 (2003) 193–202.
[50] P.J. Pollard, N.C. Wortham, I.P. Tomlinson, The TCA cycle and tumorigenesis: the examples of fumarate hydratase and succinate dehydrogenase, Ann. Med. 35 (2003) 632–639.
[51] P. Rustin, A. Rotig, Inborn errors of complex II–unusual human mitochondrial diseases, Biochim. Biophys. Acta 1553 (2002) 117–122.
[52] N. Ishii, T. Ishii, P.S. Hartman, The role of the electron transport SDHC gene on lifespan and cancer, Mitochondrion 7 (2007) 24–38.
[53] H.X. Hao, O. Khalimonchuk, M. Schraders, N. Dephoure, J.P. Bayley, H. Kunst, P. Devilee, C.W. Cremers, J.D. Schiffman, B.G. Bentz, S.P. Gygi, D.R. Winge, H. Kremer, J. Rutter, SDH5, a gene required for flavination of succinate dehydrogenase, is mutated in paraganglioma, Science 325 (2009) 1139–1142.
[54] M.A. Birch-Machin, R.W. Taylor, B. Cochran, B.A. Ackrell, D.M. Turnbull, Late-onset optic atrophy, ataxia, and myopathy associated with a mutation of a complex II gene, Ann. Neurol. 48 (2000) 330–335.
[55] T. Bourgeron, P. Rustin, D. Chretien, M. Birch-Machin, M. Bourgeois, E. Viegas-Pequignot, A. Munnich, A. Rotig, Mutation of a nuclear succinate dehydrogenase gene results in mitochondrial respiratory chain deficiency, Nat. Genet. 11 (1995) 144–149.
[56] B. Parfait, D. Chretien, A. Rötig, C. Marsac, A. Munnich, P. Rustin, Compound heterozygous mutations in the flavoprotein gene of the respiratory chain complex II in a patient with Leigh syndrome, Hum. Genet. 106 (2000) 236–243.
[57] R. Van Coster, S. Seneca, J. Smet, R. Van Hecke, E. Gerlo, B. Devreese, J. Van Beeumen, J.G. Leroy, L. De Meirleir, W. Lissens, Homozygous Gly555Glu mutation in the nuclear-encoded 70 kDa flavoprotein gene causes instability of the respiratory chain complex II, Am. J. Med. Genet. A 120 (2003) 13–18.
[58] D. Ghezzi, P. Goffrini, G. Uziel, R. Horvath, T. Klopstock, H. Lochmüller, P. D'Adamo, P. Gasparini, T.M. Strom, H. Prokisch, F. Invernizzi, I. Ferrero, M. Zeviani, SDHAF1, encoding a LYR complex-II specific assembly factor, is mutated in SDH-defective infantile leukoencephalopathy, Nat. Genet. 41 (2009) 654–656.
[59] E. Tomitsuka, H. Hirawake, Y. Goto, M. Taniwaki, S. Harada, K. Kita, Direct evidence for two distinct forms of the flavoprotein subunit of human mitochondrial complex II (succinate–ubiquinone reductase), J. Biochem. 134 (2003) 191–195.
[60] E. Tomitsuka, Y. Goto, M. Taniwaki, K. Kita, Direct evidence for expression of type II flavoprotein subunit in human complex II (succinate–ubiquinone reductase), Biochem. Biophys. Res. Commun. 311 (2003) 74–79.
[61] M. Salvi, N. Morrice, A. Brunati, A. Toninello, Identification of the flavoprotein of succinate dehydrogenase and aconitase as in vitro mitochondrial substrates of Fgr tyrosine kinase, FEBS Lett. 581 (2007) 5579–5585.
[62] H. Esumi, J. Lu, Y. Kurashima, T. Hanaoka, Antitumor activity of pyrvinium pamoate, 6-(dimethylamino)-2-[2-(2,5-dimethyl-1-phenyl-1H-pyrrol-3-yl)ethenyl]-1-me thyl-quinolinium pamoate salt, showing preferential cytotoxicity during glucose starvation, Cancer Sci. 95 (2004) 685–690.
[63] B.E. Baysal, R.E. Ferrell, J.E. Willett-Brozick, E.C. Lawrence, D. Myssiorek, A. Bosch, A. van der Mey, P.E. Taschner, W.S. Rubinstein, E.N. Myers, C.W. Richard, C.J. Cornelisse, P. Devilee, B. Devlin, Mutations in SDHD, a mitochondrial complex II gene, in hereditary paraganglioma, Science 287 (2000) 848–851.
[64] J.M. Weinberg, M.A. Venkatachalam, N.F. Roeser, I. Nissim, Mitochondrial dysfunction during hypoxia/reoxygenation and its correction by anaerobic metabolism of citric acid cycle intermediates, Proc. Natl. Acad. Sci. U. S. A. 97 (2000) 2826–2831.
[65] A. Hirayama, K. Kami, M. Sugimoto, M. Sugawara, N. Toki, H. Onozuka, T. Kinoshita, N. Saito, A. Ochiai, M. Tomita, H. Esumi, T. Soga, Quantitative metabolome profiling of colon and stomach cancer microenvironment by capillary electrophoresis time-of-flight mass spectrometry, Cancer Res. 69 (2009) 4918–4925.

Please cite this article as: C. Sakai, et al., Mitochondrial fumarate reductase as a target of chemotherapy: From parasites to cancer cells, Biochim. Biophys. Acta (2012), doi:10.1016/j.bbagen.2011.12.013

PLoS Neglected Tropical Diseases (accepted for publication, February 19, 2012)

Population structure and transmission dynamics of *Plasmodium vivax* in the Republic of Korea based on microsatellite DNA analysis

Moritoshi Iwagami[1], Megumi Fukumoto[1,2], Seung-Young Hwang[3], So-Hee Kim[4], Weon-Gyu Kho[3, 4*], Shigeyuki Kano[1, 2*]

[1] Department of Tropical Medicine and Malaria, Research Institute, National Center for Global Health and Medicine, 1-21-1 Toyama, Shinjuku, Tokyo 162-8655, Japan

[2] Graduate School of Comprehensive Human Sciences, University of Tsukuba, 1-1-1 Tennodai, Tsukuba, Ibaraki 305-8577, Japan

[3] Department of Parasitology, Inje University, College of Medicine, 633-165 Gaegum-dong, Busanjin-gu, Busan 614-735, Korea

[4] Department of Malariology, Paik Institute of Clinical Research, Inje University, College of Medicine, 633-165 Gaegum-dong, Busanjin-gu, Busan 614-735, Korea

***Corresponding authors**

Abstract

Background: In order to control malaria, it is important to understand the genetic structure of the parasites in each endemic area. *Plasmodium vivax* is widely distributed in the tropical to temperate regions of Asia and South America, but effective strategies for its elimination have yet to be designed. In South Korea, for example, indigenous vivax malaria was eliminated by the late 1970s, but re-emerged from 1993. We estimated the population structure and temporal dynamics of transmission of *P. vivax* in South Korea using microsatellite DNA markers.

Methodology/Principal Findings: We analyzed 255 South Korean *P. vivax* isolates collected from 1994 to 2008, based on 10 highly polymorphic microsatellite DNA loci of the *P. vivax* genome. Allelic data were obtained for the 87 isolates and their microsatellite haplotypes were determined based on a combination of allelic data of the loci. In total, 40 haplotypes were observed. There were two predominant haplotypes: H16 and H25. H16 was observed in 9 isolates (10%) from 1996 to 2005, and H25 in 27 (31%) from 1995 to 2003. These results suggested that the recombination rate of *P. vivax* in South Korea, a temperate country, was lower than in tropical areas where identical haplotypes were rarely seen in the following year. Next, we estimated the relationships among the 40 haplotypes by eBURST analysis. Two major groups were found: one composed of 36 isolates (41%) including H25; the other of 20 isolates (23%) including H16. Despite the low recombination rate, other new haplotypes that are genetically distinct from the 2 groups have also been observed since 1997 (H27).

Conclusions/Significance: These results suggested a continual introduction of *P. vivax* from other population sources, probably North Korea. Molecular epidemiology using microsatellite DNA of the *P. vivax* population is effective for assessing the population structure and transmission dynamics of the parasites - information that can assist in the elimination of vivax malaria in endemic areas.

Author Summary

Vivax malaria is widely prevalent, mainly in Asia and South America with 390 million reported cases in 2009. Worldwide, in the same year, 2.85 billion people were at risk. *Plasmodium vivax* is prevalent not only in tropical and subtropical areas but also in temperate areas where there are no mosquitoes in cold seasons. While most malaria researchers are focusing their studies on the parasite in tropical areas, we examined the characteristics of *P. vivax* in South Korea (temperate area) temporally, using 10 highly polymorphic microsatellite DNA (a short tandem repeat DNA sequence) in the parasite genome, and highlighted the differences between the tropical and temperate populations. We found that the South Korean *P. vivax* population had low genetic diversity and low recombination rates in comparison to tropical *P. vivax* populations that had been reported. We also found that some of the parasite clones in the population were changing from 1994 to 2008, evidence suggesting the continual introduction of the parasite from other populations, probably from North Korea. Polymorphic DNA markers of the *P. vivax* parasite are useful tools for estimating the situation of its transmission in endemic areas.

Introduction

Plasmodium vivax, the second most prevalent species of the human malaria parasite, is widely distributed around the world, especially in Asia and South America; it ranges from tropical to temperate areas [1, 2]. In these countries, the proportion of *P. falciparum* cases is gradually decreasing due to the impact of global malaria control programs such as "The Roll Back Malaria Partnership" and "The Global Fund to Fight AIDS, Tuberculosis and Malaria" as well as local control programs. In contrast, the proportion of *P. vivax* cases is gradually increasing [1], and therefore deserves more attention than it has previously received [3].

Understanding the genetic characteristics of the malaria parasite population is important for monitoring the transmission pattern and evaluating the effectiveness of malaria control in endemic areas [4-7]. Recently, the population structure and transmission dynamics of *P. vivax* have been reported in some tropical and subtropical areas where the parasites are prevalent throughout the year or seasonally prevalent but not discontinuous during the year [8-13]. However, little is known about these characteristics in temperate areas where vivax malaria is only seasonally prevalent and discontinuous during the year.

In the Republic of Korea (South Korea), which is in the temperate zone of the continent of Asia, indigenous vivax malaria had been successfully eliminated by the late 1970s thanks to an effective program conducted by the National Malaria Eradication Service of the South Korean government with the support of the WHO

[14-16], but has re-emerged since 1993 [17]. At the beginning of the re-emergence, the patients were only South Korean soldiers, veterans, and soldiers from the US military who were serving in the border area between North and South Korea in the western Demilitarized Zone (DMZ) [18-20]. Gradually, however, the number of infected civilians who lived in or near the area increased [18], suggesting local transmission of *P. vivax* between humans and *Anopheles* mosquitoes in the country. The number of vivax malaria cases increased steadily until 2000 (4,183 cases), then began to decrease gradually until 2004 (864 cases) (Fig. 1) [1, 16]. In spite of continuous malaria control measures implemented by the South Korean government, the numbers of reported cases fluctuated between 1,000 and 2,000 cases per year from 2005 to 2009 [1]. The WHO reports that vivax malaria was more prevalent in the Democratic People's Republic of Korea (North Korea), where there were 296,540 cases in 2001 and 14,845 cases in 2009 [1, 19].

We previously conducted genetic epidemiological surveys of the *P. vivax* population in South Korea using DNA sequences of some antigenic molecules of the parasite (circumsporozoite protein, Duffy binding protein, apical membrane antigen 1, merozoite surface protein-1) and found that there were 2 genotypes in the country's parasite population [21-25]. The advantage of using antigenic molecules of the parasites for genetic epidemiology is that they could be vaccine candidates; however such antigenic molecules are under strong selective pressure from the host immune system, so the variation in the molecules might be biased due to this [26]. In previous studies, the isolates that were used were collected from vivax malaria patients in a single year so temporal changes in the parasite population could not be examined. In the present study, we examined the population structure and the transmission dynamics of *P. vivax* in South Korea temporally using 10 highly polymorphic neutral DNA markers of the parasite collected from 1994 to 2008 and compared these characteristics with those reported in tropical and subtropical areas. Based on these data, we provide a possible explanation as to why it has not been possible to eliminate vivax malaria in South Korea in spite of a continuous governmental effort.

Methods

Materials

A total of 255 *P. vivax* samples isolated from South Korean soldiers or veterans who had served in the DMZ from 1994 to 2008 were used in this study. These patients were also diagnosed by microscopic examination of peripheral blood smears when they contracted malaria. The patient blood samples were collected and preserved at -30°C until use. This study was performed according to the Ethical Guidelines for Clinical Research issued by the Ministry of Health, Labour and Welfare of Japan on July 31, 2008, and the Ethical Guidelines for Epidemiological Research

issued by the Ministries of Health, Labour and Welfare, and of Education, Science, Culture, and Sports of Japan on December 1, 2008. Because of the long-term prior collection of widely distributed samples, written or oral informed consent from the patients for the specific purpose of this study could not be obtained at each sample collection. However, no author of the study was involved in gathering patient samples and the individual information of the donors was disconnected from the authors. Thus, all the samples were anonymized, and indeed it is most unlikely that the results obtained from the analysis of the isolated parasites would result in a breach of donor privacy.

DNA extraction

Parasite DNA was extracted from frozen whole blood samples by phenol-chloroform extraction after proteinase K digestion [27] or by QIAamp DNA Mini Kit (Qiagen, Valencia, CA, USA).

Genotyping by polymerase chain reaction (PCR)

Ten microsatellite DNA loci were amplified by PCR. The loci were as follows: MS1 (chromosome 3), MS4 (chromosome 6), MS5 (chromosome 6), MS6 (chromosome 11), MS7 (chromosome 12), MS8 (chromosome 12), MS9 (chromosome 8), MS12 (chromosome 5), MS15 (chromosome 5) and MS20 (chromosome 10). The PCR primer sets and amplification conditions were consistent with the protocol of Karunaweera et al. [28]. Sizes of fluorescently-labeled PCR products were measured on an Applied Biosystems Prism Genetic Analyzer 3130*xl* using GeneMapper(R) version 4.1 with a 500 ROX size standard (Applied Biosystems, CA, USA).

Amplified different-sized PCR products using the same primer sets were considered to be individual alleles within a locus, as size variation among isolates is consistent with the repeat number in a microsatellite locus [5]. The electropherogram shows peak profiles for the microsatellite loci, based on the fluorescence intensity of the labeled PCR products in this analysis. Multiple alleles per locus were scored if minor peaks were taller than at least one-third the height of the predominant allele for each locus. Multiple-genotype infections (MGIs) were defined as those in which at least one of the 10 loci contained more than one allele [5].

Population genetic analyses

Population genetic analyses were performed based on allele frequencies of the 10 microsatellite loci of the population. The level of genetic diversity of the *P. vivax* population in South Korea was assessed by allele number per locus (*A*) and expected heterozygosity (H_E). H_E values for each locus were calculated using $H_E = [n/(n - 1)] [1 - \sum p_i^2]$, where n corresponds to the number of isolates examined and p_i is the frequency of the i^{th} allele. The statistical differences among those values were evaluated by Welch's t-test.

Multilocus linkage disequilibrium (LD)

was assessed using the standardized index of association (I_A^S) [29, 30]. This analysis was performed using the LIAN 3.5 Web interface [31]. I_A^S was calculated using the formula $I_A^S = (V_D/Ve - 1)/(l - 1)$ with permutation testing of the null hypothesis of complete linkage equilibrium ($I_A^S = 0$), where V_D is the observed mismatch variance, Ve is the expected mismatch variance, and l is the number of examined loci. Significances of the observed I_A^S values were calculated by Monte-Carlo simulation, using 10,000 random permutations of the data. This statistic is a variation of the method proposed by Maynard-Smith et al [29]. The results were standardized by the number of loci, to enable a comparison of different data sets [30]. This test was applied to the data sets from each population in two ways. First, the mixed-clone infections were excluded so that only the single-clone infections were analyzed, giving absolute confidence in the haplotype profile. Second, any multilocus genotype found in more than one isolate was only counted once in the analysis, i.e. unique haplotypes only, reducing the sample size slightly and thereby removing the possible effect of recent epidemic expansion of particular clones [5].

Microsatellite haplotypes of the isolates were determined based on a combination of the allelic data of the 10 loci. The relationships among the haplotypes were estimated by eBURST analysis [32].

Results

The allelic data of the 10 microsatellite loci were obtained from 87 of the 255 (34%) isolates that were used in the study. They were not available in the remaining 168 isolates (66%) due to failure in acquiring PCR products of some loci by PCR-based genotyping. Failure was possibly due to there being only a small amount of DNA for PCR amplification or to the DNA being of low quality after multiple times of freeze-thaw.

When different sizes of alleles were observed in one locus, we regarded this as multiple genotype infections (MGIs). MGIs were observed in some of the 10 microsatellite loci in 85 of the 87 isolates (97.7%). The frequencies of MGIs varied among the 10 loci (0.00 to 0.84; average: 0.29) (Table 1). We also examined the number of MGI loci per isolate. In the 87 isolates with 10 loci, the highest frequency of MGI loci per isolate was 2 (25 isolates) and the frequencies decreased gradually according to the increase in the number of MGI loci (Fig. 2). The highest number of MGI loci per isolate was 8 (one isolate). The major alleles in each locus were used for population genetic analysis.

Genetic diversity

In the 10 loci, the number of alleles (A) for each locus was 2 to 7 (average: 4.3). The expected heterozygosity (H_E) for each of these loci was 0.05 to 0.66 (average: 0.43) (Table 2).

Next, the *P. vivax* population was divided into 2 groups: one comprised of the 47 isolates collected from 1994 to 2000 when the numbers of vivax malaria cases

increased; the other comprised of the 40 isolates collected from 2001 to 2008, when the numbers of cases decreased until 2004 and then increased slightly. The level of genetic diversity was reassessed for each group. For the first group, the averages ± SE of *A* and H_E were 2.70 ± 0.26 and 0.36 ± 0.06, respectively. For the second group, the averages ± SE of *A* and H_E were 3.80 ± 0.57 and 0.50 ± 0.10, respectively (Fig. 1). The levels of genetic diversity were relatively higher in the second group, with *P* values at 0.11 and 0.24 for average *A* and average H_E, respectively.

Furthermore, we also divided the population into 3 groups, each covering 5-year periods: 1994 to 1998 (33 isolates), 1999 to 2003 (36 isolates) and 2004 to 2008 (18 isolates). The level of genetic diversity was reassessed for each group (Fig. 3). For the first group, the averages ± SE of *A* and H_E were 2.50 ± 0.27 and 0.31 ± 0.05, respectively. For the second group, the averages ± SE of *A* and H_E were 3.00 ± 0.42 and 0.42 ± 0.09, respectively. For the third group, the averages ± SE of *A* and H_E were 3.80 ± 0.57 and 0.56 ± 0.10, respectively. The levels of genetic diversity gradually increased with *P* values at 0.06 and 0.05 if we compared the difference of the average *A* between the first group (1994-1998) and the third group (2003-2008) and the difference of the average H_E between the first and the third group, respectively.

Multilocus Linkage disequilibrium (LD)

Likewise, the analysis of genetic diversity, I_A^S values were also calculated for the two populations: one comprised the isolates collected from 1994 to 2000 and the other comprised the isolates collected from 2001 to 2008, with permutation testing of the null hypothesis of $I_A^S = 0$ (equilibrium of multilocus frequencies) (Table 3). When the single-clone haplotype was used in the analysis, the I_A^S values of the former (1994-2000) and the latter (2001-2008) were 0.529 and 0.218, respectively, whereas when the unique haplotypes were used in the analysis, those of the former and the latter were 0.346 and 0.173, respectively. Significant linkage disequilibrium was observed in both populations ($P < 0.001$).

Similar to the analyses of genetic diversity, we also divided the population into 3 groups covering 5-year periods: 1994 to 1998 (33 isolates), 1999 to 2003 (36 isolates) and 2004 to 2008 (18 isolates). The I_A^S values were also calculated for each group. When the single-clone haplotype was used in the analysis, the I_A^S values of the first (1994-1998), the second (1999-2003) and the third (2004-2008) groups were 0.584, 0.315 and 0.140, respectively, whereas when the unique haplotypes were used in the analysis, those of the first, the second and the third were 0.408, 0.231 and 0.153, respectively (Table 4). Significant linkage disequilibrium was observed in both populations ($P < 0.001$).

Haplotypes and the relationships among the haplotypes

Microsatellite haplotypes of the 87 isolates were determined based on a combination of the allelic data of the 10 microsatellite loci; 40 haplotypes (H1-H40)

were observed (Table 5). There were 2 major haplotypes (H16 and H25): H16 was observed in 9 isolates (10%) out of the 87 isolates in samples collected from 1996 to 2005; H25 was observed in 27 isolates (31%) out of the 87 isolates in samples collected from 1995 to 2003. H16 and H25 share only 3 alleles in the loci, MS8, MS12 and MS20, but those in 7 other loci were different from each other.

The relationships among the 40 haplotypes were estimated by eBURST analysis [32] with the following criterion: when 2 isolates shared more than 7 identical loci out of the 10 loci, they were connected with a branch (Fig. 4). Again, two major groups were found: Group 1 was composed of 36 isolates (41%) including the isolates with H25; Group 2 was composed of 20 isolates (23%) including those with H16. Some new or isolated haplotypes, namely H5, H6, H7, H8, H11, H12, H19, H31, H32, H33, H35, H36, that were not included in the 2 major groups or connected to any other haplotypes, have also been observed since 1998. H6 and H7 were not shown in Figure 2 because these haplotypes were quite different from the other haplotypes.

Discussion

This is the first 15-year-long longitudinal study on *P. vivax* population genetics using highly polymorphic neutral markers. The present study demonstrated that the level of genetic diversity of the *P. vivax* population in South Korea was remarkably lower than the levels in tropical and subtropical areas reported by Karunaweera et al. [28] and Orjuela-Sánchez et al. [33] (Table 2). The 10 microsatellite loci used in the present study were a subset of the 14 loci used in the previous studies by other groups [28, 33]. Imwong et al. also reported that the mean values of H_E of *P. vivax* populations from Thailand (n=28), India (n=27) and Colombia (n=27) were 0.77, 0.76 and 0.64, respectively [11], using 11 other microsatellite loci in the genome. These values reported by Imwong et al. were also higher than those in South Korea. .

Sample size (n) and sampling conditions such as the size of sampling area and the length of sampling period may affect levels of genetic diversity of living organisms. In comparison to other studies the sample size of the present study (n=87) was relatively large and the sampling period (15 years: from 1994 to 2008) was relatively long [11, 28, 33]. Generally, one would expect to see an increase in the level of genetic diversity when these conditions (a large number of samples and a long sampling period) are present. However, the South Korean *P. vivax* population showed low levels of genetic diversity, suggesting that the effective size of the re-emerged *P. vivax* population in South Korea might be small.

Microsatellite variation is strongly dependent on the length of repeat arrays [34]. Studies of numerous organisms have shown higher levels of variation in loci with long repeat arrays than those with short repeat arrays [35]. In the present study, however, even the locus with a long